Article

Development of a Sustainable Process for Complex Sulfide Ores Containing Anglesite: Effect of Anglesite on Sphalerite Floatability, Enhanced Depression of Sphalerite by Extracting Anglesite, and Recovery of Extracted Pb^{2+} as Zero-Valent Pb by Cementation Using Zero-Valent Fe

Kosei Aikawa [1],[*] , **Mayumi Ito [2]** , **Atsuhiro Kusano [1]** , **Sanghee Jeon [2]** , **Ilhwan Park [2]** and **Naoki Hiroyoshi [2]**

[1] Division of Sustainable Resources Engineering, Graduate School of Engineering, Hokkaido University, Sapporo 060-8628, Japan; e531taikoteam@gmail.com

[2] Division of Sustainable Resources Engineering, Faculty of Engineering, Hokkaido University, Sapporo 060-8628, Japan; itomayu@eng.hokudai.ac.jp (M.I.); shjun1121@eng.hokudai.ac.jp (S.J.); i-park@eng.hokudai.ac.jp (I.P.); hiroyosi@eng.hokudai.ac.jp (N.H.)

[*] Correspondence: k-aikawa@frontier.hokudai.ac.jp; Tel.: +81-11-706-6315

Abstract: The presence of anglesite ($PbSO_4$) in complex sulfide ores negatively affects the separation of Cu-Pb sulfides and sphalerite (ZnS) due to lead activation, and $PbSO_4$ rejected to tailings dams contaminates the surrounding environment with lead. To address these problems, this study investigated the application of ethylene diamine tetra acetic acid (EDTA) pretreatment extracting $PbSO_4$ to ZnS flotation and the recovery of the extracted Pb^{2+} as zero-valent Pb by cementation using zero-valent iron (ZVI). The application of EDTA pretreatment could extract ~99.8% of $PbSO_4$, thus depressing ZnS floatability from 82% to 30%. In addition, cementation using ZVI could recover ~99.7% of Pb^{2+} from the leachate of EDTA pretreatment.

Keywords: flotation; complex sulfide ores; sphalerite; anglesite; extraction; cementation

1. Introduction

In 2015, 193 governments adopted 17 sustainable development goals (SDGs) aiming to eradicate poverty, protect the planet, and ensure peaceful and prosperous lives for everyone by 2030 [1–3]. Number 13 of the SDGs—"Climate Action"—envisions drastic carbon dioxide (CO_2) emission reductions to combat climate change and achieve a carbon-neutral society by 2050 [4]. Copper (Cu), lead (Pb), and zinc (Zn) are classified as critical metals defined by the World Bank as essential in renewable energy and clean storage technologies (e.g., wind turbines, solar photovoltaic (PV) panels, batteries, etc.), and thus their demands are projected to significantly increase in the future to achieve a carbon-neutral society [5,6].

Complex sulfide ores, some of the most important sources of critical metals, are typically composed of several metal sulfide minerals such as chalcopyrite ($CuFeS_2$), galena (PbS), and sphalerite (ZnS). In the mineral processing of complex sulfide ores consisting of Cu-Pb-Zn sulfide minerals, flotation has been commonly adopted to produce concentrates of each mineral [7–16]. Some complex sulfide ores contain not only PbS but also anglesite ($PbSO_4$), the presence of which is problematic for the separation of Cu, Pb, and Zn by flotation due to the unwanted activation of ZnS by Pb^{2+} released from $PbSO_4$ [17–19]. In the general flotation circuit of Cu-Pb-Zn sulfide ores, Cu and Pb sulfides are first recovered as froth, and then ZnS is recovered with the assistance of activators (e.g., $CuSO_4$) [20,21]. When $PbSO_4$ is contained in complex sulfide ores, however, Pb^{2+} is readily released from $PbSO_4$ during conditioning and/or flotation due to its higher solubility compared to PbS—the solubility product (K_{sp}) of $PbSO_4$ and PbS is $10^{-7.79}$ and $10^{-26.77}$, respectively [22]—and

activates the surface of ZnS via the formation of PbS-like compounds, as illustrated in Equation (1) [23,24];

$$ZnS(s) + Pb^{2+} = PbS(s) + Zn^{2+} \tag{1}$$
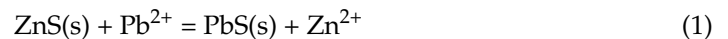
The activation of ZnS by Pb^{2+} is known to increase the ZnS floatability because of a higher affinity of PbS-like compounds for xanthate compared to ZnS [25–27]. As a result, ZnS is recovered as froth together with $CuFeS_2$ and PbS, making their separation difficult [17]. Therefore, a proper way of depressing ZnS floatability during flotation of complex sulfide ores containing $PbSO_4$ should be established.

In addition, $PbSO_4$ is typically distributed into flotation tailings because it has poor affinity for the collector (e.g., xanthate) [28,29]. The disposal of $PbSO_4$ into tailings storage facilities (TSFs) would cause lead pollution in the surrounding environment [30,31]. That is, the presence of $PbSO_4$ in complex sulfide ores would cause not only difficulties in the separation of ZnS from Cu and Pb sulfide minerals but also lead pollution in the surrounding environment of TSFs.

To address the above-mentioned problems, this study investigated the improvement of ZnS depression by extracting $PbSO_4$ and the recovery of extracted Pb^{2+} as zero-valent Pb by cementation using zero-valent iron (ZVI). Specifically, this study was devoted not only to optimizing the conditions for the extraction of $PbSO_4$ by ethylene diamine tetra acetic acid (EDTA) as well as the recovery of extracted Pb^{2+} as Pb^0 via cementation using ZVI but also to understanding how the absence/presence of $PbSO_4$ affected the floatability of ZnS through flotation experiments and surface characterizations of $ZnS/PbSO_4$ mixtures with and without EDTA pretreatment. Finally, a sustainable flowsheet for the processing of complex sulfide ores containing $PbSO_4$ with the combination of EDTA pretreatment, flotation, and cementation is proposed.

2. Materials and Methods

2.1. Minerals and Reagents

Five types of minerals were used in this study: sphalerite (ZnS, Kamioka Mine, Hida, Japan), lead sulfate ($PbSO_4$, 98% purity), lead carbonate ($PbCO_3$, 99% purity), lead chloride ($PbCl_2$, 99% purity), and quartz (SiO_2, 99% purity). The lead compounds and quartz were obtained from FUJIFILM Wako Pure Chemical Corporation (Osaka, Japan). A mineral specimen of ZnS was characterized using X-ray fluorescence spectroscopy (XRF, EDXL300, Rigaku Corporation, Tokyo, Japan) and X-ray powder diffraction (XRD, MultiFlex, Rigaku Corporation, Tokyo, Japan), and its chemical and mineralogical compositions ware shown in Table 1 and Figure 1, respectively. The XRD pattern of ZnS implied that ZnS was relatively pure due to the absence of the peaks of common minerals such as SiO_2. In preparation for the flotation experiments, ZnS was ground by a vibratory disc mill (RS 200, Retsch Inc., Haan, Germany) and screened to obtain a size fraction of $-75 + 38$ µm.

Table 1. Chemical composition of a mineral specimen of ZnS based on XRF.

Elements	Zn	Fe	Pb	S	Si
Mass fraction (%)	55.7	6.2	0.2	21.3	8.4

For the flotation experiments, potassium amyl xanthate (KAX, Tokyo Chemical Industry Co., Ltd., Tokyo, Japan) and methyl isobutyl carbinol (MIBC, FUJIFILM Wako Pure Chemical Corporation, Osaka, Japan) were used as collector and frother, respectively. Zinc sulfate ($ZnSO_4$) and sodium sulfite (Na_2SO_3), purchased from FUJIFILM Wako Pure Chemical Corporation (Osaka, Japan), were used as depressants for ZnS. Sulfuric acid (H_2SO_4, FUJIFILM Wako Pure Chemical Corporation, Osaka, Japan) and sodium hydroxide (NaOH, FUJIFILM Wako Pure Chemical Corporation, Osaka, Japan) were used as pH adjusters. For the extraction experiments, ethylene diamine tetra acetic acid (EDTA, FUJIFILM Wako Pure Chemical Corporation, Osaka, Japan) was used as an extractant. For the cementation

experiments, zero-valent Fe (ZVI) powder (Fe^0, −45 μm, FUJIFILM Wako Pure Chemical Corporation, Osaka, Japan) was used as a reductant.
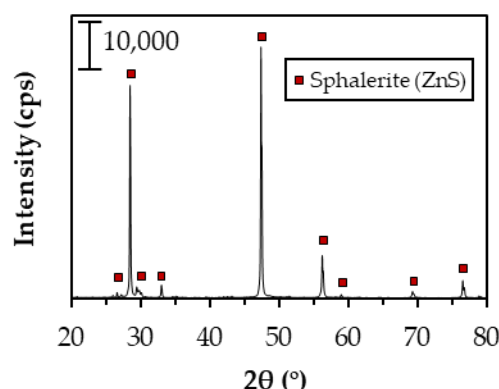
Figure 1. XRD pattern of a mineral specimen of ZnS.

2.2. Experimental Methods

2.2.1. Extraction Experiments of Lead Minerals Using EDTA

The extraction experiments of lead minerals were conducted in 50 mL Erlenmeyer flasks containing 1 g of the lead mineral and an EDTA solution (solid/liquid ratio: 1 g/10 mL). The solutions containing 100, 200, or 500 mM EDTA were used without pH adjustment (natural pH: 11.3). The flasks were shaken in a thermostat water bath shaker at a shaking speed of 120 rpm and an amplitude of 40 mm at 25 °C. After this, the leachates were collected by filtration using 0.2 μm syringe-driven membrane filters and immediately analyzed using an inductively coupled plasma atomic emission spectrometer (ICP-AES, ICPE 9820, Shimadzu Corporation, Kyoto, Japan) (margin of error = ±2%) to measure the concentration of Pb^{2+}. The experiments were performed in triplicate to ascertain that the differences observed were statistically significant, and the extraction efficiency of the lead mineral (E_{Pb}) was calculated using the following equation:

$$E_{Pb} = \frac{[Pb]_i}{[Pb]_{tot}} \times 100 \tag{2}$$

where $[Pb]_{tot}$ and $[Pb]_i$ are total Pb (mM) and extracted Pb (mM), respectively.

2.2.2. Cementation Experiments of the Extracted Pb^{2+}

The cementation experiments of Pb^{2+} extracted from $PbSO_4$ were conducted in 50 mL Erlenmeyer flasks. A volume of 10 mL of the leachate collected by filtration using 0.2 μm syringe-driven membrane filters after the extraction experiments ([EDTA], 500 mM; S/L ratio, 1 g/10 mL; time, 30 min) was added to the flask, and ultrapure nitrogen gas (N_2; 99.99%) was introduced for 15 min to remove the dissolved oxygen (DO) present in the leachate. Then, a known amount of ZVI powder was added to the flask, and N_2 was further introduced for 5 min. The flask was tightly capped with a silicon rubber plug and parafilm and shaken in a thermostat water bath shaker at a shaking speed of 120 rpm and an amplitude of 40 mm at 25 °C. After this, the leachate was filtered using a 0.2 μm syringe-driven membrane filter, and the filtrate was immediately analyzed using ICP-AES to measure the concentration of Pb^{2+}. Meanwhile, the residue was washed thoroughly with distilled water, dried in a vacuum-drying oven at 40 °C, and analyzed by scanning electron microscopy with energy-dispersive X-ray spectroscopy (SEM-EDS, JSM-IT200TM, JEOL Co., Ltd., Tokyo, Japan). The experiments were performed in triplicate to ascertain that the differences observed were statistically significant. Pb recovery (R_{Pb}) was calculated using the following equation:

$$R_{Pb} = \frac{[Pb]_I - [Pb]_F}{[Pb]_I} \times 100 \tag{3}$$

where $[Pb]_I$ and $[Pb]_F$ are the initial and the final concentrations of Pb (mM) in the leachate, respectively.

2.2.3. Flotation Experiments

The flotation experiments were carried out using an agitator-type flotation machine (ASH-F30H, Kankyo-kanri Engineering, Akita, Japan) equipped with a 400 mL flotation cell under the following conditions: pH, 6.5; temperature, 25 °C; pulp density, 5%; impeller speed, 1000 rpm; air flow rate, 1 L/min. In a 500 mL beaker, a model sample containing 15 g of ZnS and 5 g of $PbSO_4$ or SiO_2 was suspended in 300 mL of distilled water, and the supernatant was decanted to remove fine particles (<38 μm) [17]. After desliming, a model sample was repulped to 400 mL with distilled water in the flotation cell and conditioned for 3 min after adding the following reagents in sequence: ~5 kg/t of $ZnSO_4$ (100 ppm Zn^{2+}), 1 kg/t of Na_2SO_3, 20 g/t of KAX, and 20 μL/L of MIBC. Afterwards, air was introduced at a flowrate of 1 L/min, and froth was recovered for 3 min. The recovered froth/tailing products were dried at 105 °C for 24 h and analyzed by XRF to determine the recovery of Zn. The experiments were performed in duplicate to ascertain that the differences observed were statistically significant. An aliquot of the pulp of about 5 mL was collected 3 min after adding the depressant, filtered through a 0.2 μm syringe-driven membrane filter, and immediately analyzed using ICP-AES to check the extent of lead activation of ZnS. Meanwhile, the collected residues were washed thoroughly with distilled water, dried in a vacuum-drying oven at 40 °C, and analyzed by X-ray photoelectron spectroscopy (XPS, JPS-9200, JEOL Co., Ltd., Tokyo, Japan). The XPS analysis was conducted using an Al Kα X-ray source (1486.7 eV) operated at 100 W (voltage = 10 kV; current = 10 mA) under ultrahigh vacuum conditions (~10^{-7} Pa). The binding energies of photoelectrons were calibrated using C1s (285 eV) or $Zn2p_{3/2}$ (1022.0 eV) for charge correction. The XPS data were analyzed by Casa XPS, and deconvolutions of the spectra were carried out using an 80% Gaussian–20% Lorentzian peak model and a Shirley background [32–35].

In addition, flotation experiments of $ZnS/PbSO_4$ mixture after EDTA pretreatment were conducted to check how effective the removal of $PbSO_4$ was on the depression of ZnS floatability. A mixture of 15 g ZnS and 5 g $PbSO_4$ was mixed with 200 mL of a 500 mM EDTA solution (i.e., solid/liquid ratio: 20 g/200 mL) and shaken in a thermostat water bath shaker at a shaking speed of 120 rpm and an amplitude of 40 mm at 25 °C for 30 min. After this, the leachate was filtered using a 0.2 μm syringe-driven membrane filter, the filtrate was immediately analyzed using ICP-AES to measure the concentration of Pb^{2+}, and the cementation experiments to recover the extracted Pb^{2+} in the filtrate were carried out using 1 g/10 mL of ZVI for 24 h under the same conditions and with the same procedures mentioned in Section 2.2.2. Meanwhile, the residue obtained after EDTA pretreatment was washed thoroughly with distilled water and deslimed to remove fine particles [17]. After desliming, the residue was repulped to 400 mL with distilled water, and then flotation was conducted under the same conditions mentioned above. An aliquot of the pulp of about 5 mL was also collected 3 min after adding the depressant ($ZnSO_4$) and filtered through a 0.2 μm syringe-driven membrane filter, and the filtrate and residue were analyzed by ICP-AES and XPS, respectively.

3. Results and Discussion

3.1. Effects of $PbSO_4$ on ZnS Floatability

Figure 2 shows the flotation results of ZnS mixed with SiO_2 or $PbSO_4$. As can be seen, Zn recovery in the presence of SiO_2 was ~12% but significantly increased to >80% when $PbSO_4$ was present. It was reported that the affinity between ZnS and xanthate is poor, so the surface of ZnS needs to be modified using activators [21]. Since the solubility of $PbSO_4$ is higher than that of PbS, a substantial amount of Pb^{2+} might be released into the pulp during the conditioning process when the ore contains $PbSO_4$ [17]. As a result, lead activation of ZnS could occur (Equation (1)), thus increasing its floatability due to the formation of PbS-like compounds, having a higher affinity for xanthate than ZnS, on the mineral surface.

In short, the presence of $PbSO_4$ in the complex sulfide ores would negatively affect the separation of Cu-Pb from Zn. In addition, some portion of $PbSO_4$ will remain undissolved and be rejected as tailings due to the poor affinity of $PbSO_4$ for the collector (e.g., xanthate), which can cause lead contamination of the surrounding environment [28,29,36].
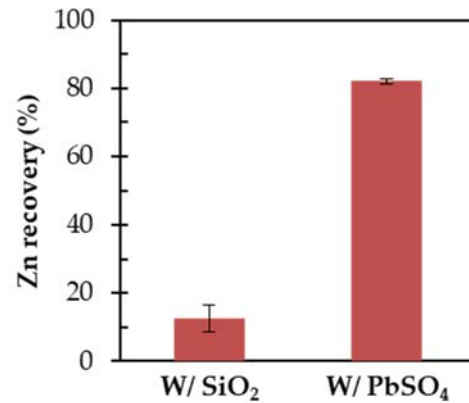
Figure 2. Flotation results of ZnS with SiO_2 or $PbSO_4$.

3.2. Extraction of PbSO₄ Using EDTA

To address the above-mentioned problems caused by the presence of $PbSO_4$ (i.e., unwanted activation of ZnS and lead contamination), its extraction prior to flotation was investigated. Among the extractants, EDTA was chosen in this study because of its ability to extract metal ions from sulfates like $PbSO_4$, without dissolving metal sulfides (e.g., PbS and ZnS) [37–40].

Figure 3a shows the extraction efficiency of $PbSO_4$ after 24 h with different concentrations of EDTA (100, 200, or 500 mM). When the stoichiometric ratio of EDTA/$[Pb]_{tot}$ was lower than 1, the amount of Pb^{2+} extracted was identical to the concentration of EDTA, which indicated that Pb^{2+} and EDTA formed a 1:1 complex (i.e., $[Pb(EDTA)]^{2-}$). When the stoichiometric ratio of EDTA/$[Pb]_{tot}$ was >1, almost all $PbSO_4$ (~98%) was extracted. The rate of $PbSO_4$ extraction was further studied with 500 mM EDTA, and the result showed that ~97% of $PbSO_4$ was extracted within 30 min (Figure 3b). EDTA could extract not only $PbSO_4$ but also other Pb minerals like $PbCO_3$ and $PbCl_2$ (Figure 4). These minerals are also unfloatable and will be rejected into the TSFs, indicating that their presence in the ores may result in the contamination of the TSFs with Pb. It was confirmed that EDTA pretreatment can extract almost all Pb minerals except for PbS, thus suppressing lead pollution to the surrounding environment of TSFs. It is noted that the concentration of EDTA should be chosen in the consideration of the amount of soluble minerals contained in ores, because EDTA would be consumed not only by Pb^{2+} but also by other metal ions from soluble minerals such as sulfates, oxides, hydroxides, and carbonates.
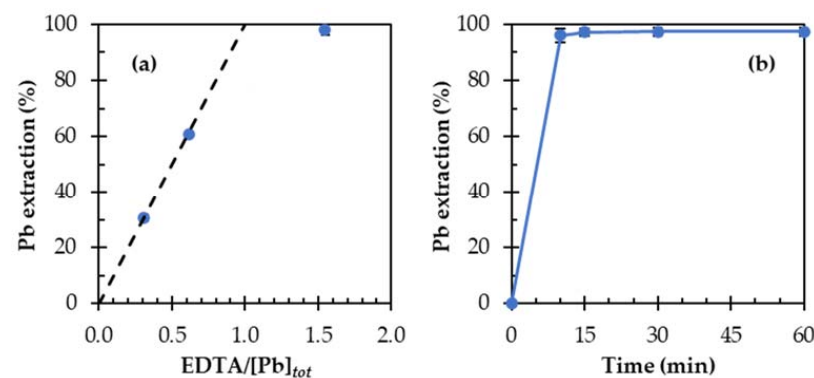
Figure 3. (**a**) Extraction efficiency of $PbSO_4$ after 24 h with different concentrations of EDTA (100, 200, or 500 mM) and (**b**) effect of time on $PbSO_4$ extraction with 500 mM EDTA. Note that the dotted line in Figure 3a corresponds to the ratio of EDTA/$[Pb]_{tot}$.
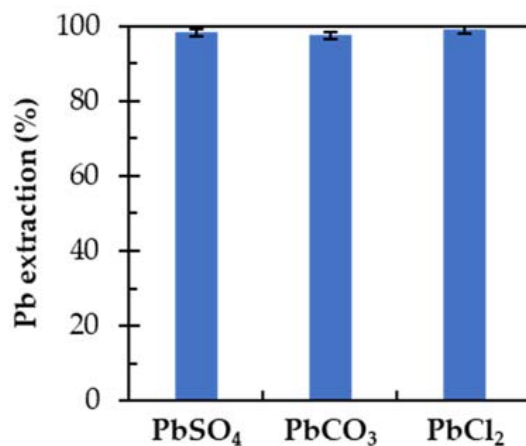
Figure 4. Extraction efficiency of lead minerals with 500 mM EDTA after 24 h.

3.3. Recovery of Extracted Pb^{2+} as Zero-Valent Pb by Cementation

After EDTA pretreatment, the recovery of Pb^{2+} from the leachate will not only add economic value but also protect the environment. Cementation is one of the effective methods to recover metal ions as zero-valent metals [41–45]. A general cementation reaction is illustrated in Equation (4): a metal (A^0) gives electrons to metal ion (B^{b+}), driven by the difference in standard redox potentials of the interacting metals and their ions, and as a result, B^{b+} is deposited on the surface of A^0 as B^0 [46–49]:

$$n\,A^0 + m\,B^{b+} \rightarrow n\,A^{a+} + m\,B^0 \ (na = mb) \tag{4}$$
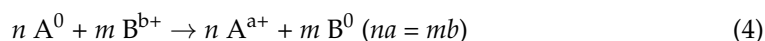
To recover the extracted Pb^{2+} as zero-valent Pb (Pb^0) from the EDTA leachate, cementation experiments were carried out using ZVI powder as a reductant after removing DO from the solution by purging with ultrapure nitrogen gas. Figure 5a shows the effects of the ZVI amount on the recovery of the extracted Pb^{2+} from the leachate after EDTA pretreatment using 500 mM EDTA for 30 min. When the amount of ZVI was 0.5 g/10 mL, ~40% of Pb^{2+} was recovered, although ~0.18 g/10 mL ZVI was stoichiometrically sufficient to recover all Pb^{2+} in the solution. As the cementation reaction progressed, the surface of ZVI was covered with cementation products (i.e., Pb^0), which hindered a further cementation reaction. This was probably the reason why 1 g/10 mL of ZVI was required to recover all Pb^{2+} from the EDTA leachate.
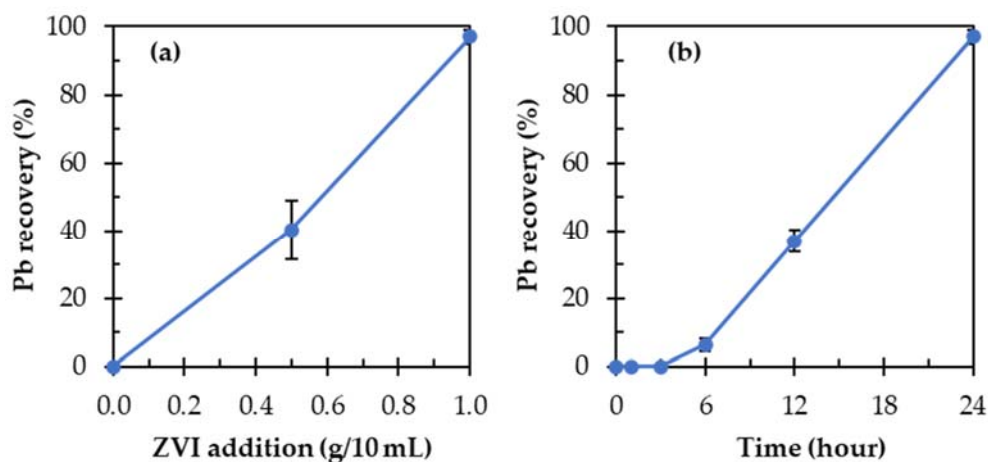
Figure 5. (**a**) Effects of the ZVI amount on the recovery of the extracted Pb after 24 h in the leachate after $PbSO_4$ extraction using 500 mM of EDTA for 30 min and (**b**) effects of time on the recovery of the extracted Pb^{2+} using 1 g/10 mL of ZVI in the leachate after EDTA pretreatment using 500 mM EDTA for 30 min.

Figure 5b shows the cementation results of Pb^{2+} by ZVI in time. As can be seen, almost no cementation occurred for 3 h, and then Pb^{2+} started being cemented gradually. The initial slow rate of Pb cementation can have two reasons: (i) the presence of Fe oxide films formed on the ZVI surface that limited the cementation of Pb^{2+} and (ii) an excess amount of free EDTA that redissolved the cemented Pb^0. After 3 h, the concentration of free EDTA ligands was most likely decreased due to its consumption in dissolving Fe oxide films and/or in forming complexes with Fe species released by the cementation reaction. It is important to note that after 24 h, ~97% cementation was achieved. To confirm the recovery of Pb^{2+} on ZVI, the residue obtained from the cementation experiment using 1 g/10 mL of ZVI for 24 h was analyzed using SEM-EDS. As shown in Figure 6, the deposition of Pb compounds on ZVI powder was observed, suggesting that the extracted Pb^{2+} was reductively deposited via the cementation reaction:

$$Pb(EDTA)^{2-} + Fe^0 = Pb^0 + EDTA + Fe^{2+} \tag{5}$$
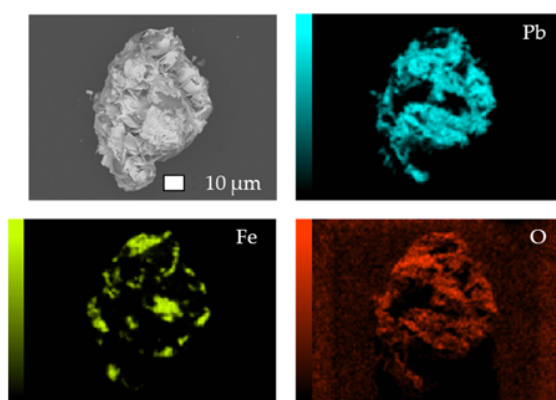
Figure 6. SEM photomicrograph of the residue of the cementation experiment using 1 g/10 mL of ZVI for 24 h with the corresponding elemental maps of Fe, Pb, and O.

Equation (5) consists of two half-cell reactions [50]:

$$Pb(EDTA)^{2-} + 2e^- = Pb^0 + EDTA^{4-} \tag{6}$$

$$Fe^0 = Fe^{2+} + 2e^- \tag{7}$$

The above-mentioned residue was also analyzed by XRD to further characterize Pb compounds formed on ZVI (Figure 7). As shown in the XRD pattern, the peaks of Fe^0, Fe_2O_3, Pb^0, and PbO were detected, indicating that Pb^{2+} was reductively deposited as Pb^0 on the surface of ZVI, as illustrated in Equation (5). The presence of PbO and Fe_2O_3 was due most likely to the oxidation of Pb^0 and ZVI surface during drying and storing of the sample [51–53].
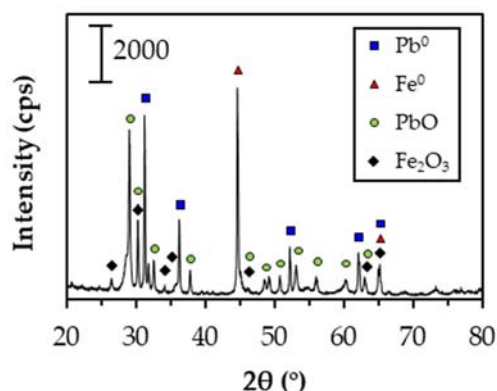
Figure 7. XRD pattern of the residue of the cementation experiment using 1 g/10 mL of ZVI for 24 h.

3.4. Effects of EDTA Pretreatment on ZnS Depression in Flotation

As described in Section 3.2, almost all PbSO$_4$ was extracted with EDTA, so the effects of EDTA pretreatment on ZnS depression in flotation were investigated. Flotation experiments using model samples (ZnS/PbSO$_4$ mixture) with and without EDTA pretreatment were conducted (Figure 8). Prior to the flotation experiments, the mixture of 15 g ZnS and 5 g PbSO$_4$ was treated with 500 mM of EDTA for 30 min (solid/liquid ratio: 20 g/200 mL), and ~99.8% of PbSO$_4$ was extracted. The cementation experiments using 1 g/10 mL of ZVI for 24 h were also carried out to recover the extracted Pb^{2+} in the filtrate obtained after EDTA pretreatment, and ~99.7% of the extracted Pb^{2+} was recovered. Meanwhile, the residue obtained after EDTA pretreatment was deslimed and repulped to 400 mL with distilled water in the flotation cell, and then the flotation experiments were conducted with ~5 kg/t of ZnSO$_4$ (100 ppm Zn^{2+}) and 1 kg/t of Na$_2$SO$_3$ as depressants at pH 6.5. As shown in Figure 8, the floatability of Zn was clearly depressed from ~82% to ~30% when EDTA pretreatment was applied.
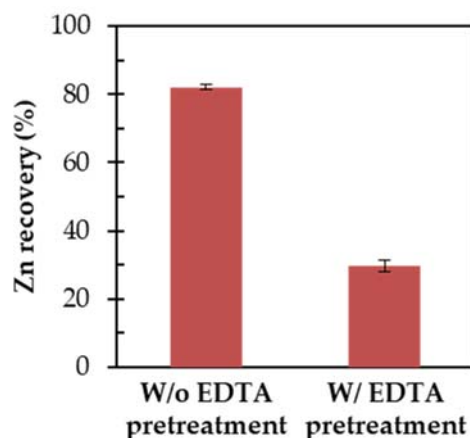
Figure 8. Effects of EDTA pretreatment on the floatability of ZnS in the presence of PbSO$_4$.

To confirm the depression of ZnS floatability after EDTA pretreatment, a pretreated sample reacted with zinc sulfate for 3 min, a ~5 mL aliquot of the pulp, was collected, and the filtrate and the residue were analyzed by ICP-AES and XPS, respectively. The concentration of Pb^{2+} in the filtrate without EDTA pretreatment was 5.3 ppm; it decreased to 0.2 ppm with EDTA pretreatment. On the other hand, the concentrations of Zn^{2+} in the filtrates with and without EDTA pretreatment were 101 and 99.4 ppm, respectively. Based on thermodynamics calculations using Equation (8), the possibility of lead activation of ZnS (Equation (1)) could be evaluated using the measured values of Pb^{2+} and Zn^{2+} [17,54,55]. In this study, the changes in free energy were calculated using measured values of Pb^{2+} and Zn^{2+} concentrations.

Table 2 shows the calculated results of the changes in free energy based on the equilibrium constants of lead activation of ZnS (Equation (1)). The change in free energy without EDTA pretreatment was negative, while that with EDTA pretreatment was positive. When the change in free energy is positive, the reverse reaction of lead activation (Equation (1)) would occur spontaneously, indicating that lead activation would be limited by EDTA pretreatment. These results support the flotation results that the depression of ZnS floatability was achieved by the pretreatment, which decreased Pb^{2+} concentration during flotation by extracting PbSO$_4$ in advance.

$$\Delta G = -RT \ln K + \ln\left(Zn^{2+}/Pb^{2+}\right) \tag{8}$$

$$K = \frac{K_{sp}^{ZnS}}{K_{sp}^{PbS}} \tag{9}$$

Table 2. Calculation results of the change in free energy with and without EDTA pretreatment.

K	ΔG (kJ/mol) Without EDTA Pretreatment	ΔG (kJ/mol) With EDTA Pretreatment
1000 [a]	−6.9	1.8
704 [b]	−6.1	2.7
1059 [c]	−7.1	1.7
1127 [d]	−7.2	1.5

[a] The equilibrium constant was obtained from a previous study [54]. [b, c, d] The equilibrium constants were calculated using Equation (9) by the reported K_{sp} values of *ZnS* and *PbS*, respectively [56–58].

To confirm whether the lead activation of sphalerite was limited by the extraction of PbSO$_4$ using EDTA, untreated ZnS as well as ZnSO$_4$-pretreated ZnS/PbSO$_4$ mixtures with and without EDTA pretreatment were analyzed by XPS. The Pb4f$_{7/2}$ core-level spectra of the samples are shown in Figure 9, and the corresponding curve-fitting parameters are summarized in Table 3. Since the Zn3s peak overlapped with the Pb4f$_{7/2}$ signals, the spectrum was resolved by curve fitting to subtract the area due to the Zn3s peak [55,59]. As illustrated in Figure 9b and c, the deconvoluted XPS spectra of the residues with and without PbSO$_4$ extraction showed two types of Pb species: (1) Pb^{2+}—S of PbS (143.6 and 138.6 eV) and (2) Pb^{2+}—SO$_4$ of PbSO$_4$ (144.7 and 139.8 eV), while the deconvoluted XPS spectrum of untreated ZnS showed no Pb species (Figure 9a) [26,60]. The decrease in the intensity of Pb^{2+}—SO$_4$ was in a good agreement with the extraction efficiency of PbSO$_4$ using EDTA for the ZnS/PbSO$_4$ mixture (~99.8%). When EDTA pretreatment was applied prior to the flotation experiments, the peak intensity ratio of PbS/ZnS decreased from 2.3 to 0.2, indicating that EDTA pretreatment was effective in limiting lead activation of ZnS. This is in line with the calculated results of the change in free energy based on thermodynamics (Table 2).
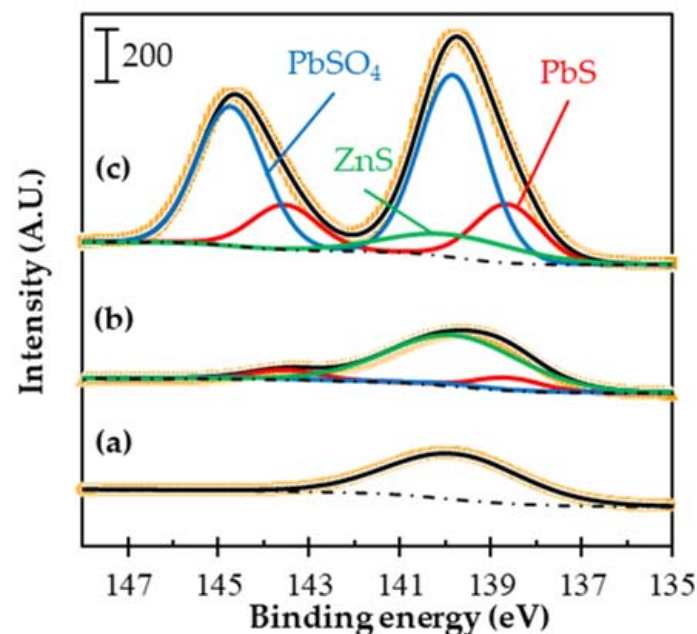
Figure 9. XPS Pb4f7/2 spectra of (**a**) raw ZnS, (**b**) ZnS/PbSO$_4$ with EDTA pretreatment, and (**c**) ZnS/PbSO$_4$ without EDTA pretreatment.

Table 3. XPS peak parameters for Pb4f$_{7/2}$ spectra and relative abundances of Pb species.

Binding Energy (eV)	FWHM	Assignments	Contents (at.%)		
			Untreated [a]	W/ EDTA [b] Pretreatment	W/o EDTA [a] Pretreatment
138.6 ± 0.05 143.5 ± 0.05	1.7	PbS	0	17.1	21.5
139.8 ± 0.05 144.7 ± 0.05	1.7	PbSO$_4$	0	8.8	48.4
139.8 ± 0.05	3.4	ZnS	100	80.5	9.5

[a] The binding energies of photoelectrons were calibrated using C1s (285 eV) for charge correction. [b] The binding energies of photoelectrons were calibrated using Zn2p$_{3/2}$ (1022.0 eV) for charge correction.

3.5. Implication of This Study

The results of this study have significant implications not only for understanding how the presence of PbSO$_4$ in complex sulfide ores affects the floatability of ZnS but also for proposing a sustainable process flowsheet covering both the improved flotation separation of complex sulfide ores and the detoxification of solid/solution wastes contaminated with Pb species. Firstly, the presence of PbSO$_4$ might have a detrimental impact on the flotation separation of complex sulfide ores due to unwanted lead activation of ZnS that improves its floatability, which could not be depressed with ZnSO$_4$—the conventional depressant for ZnS. Secondly, EDTA washing could extract almost all PbSO$_4$ from the ZnS/PbSO$_4$ mixture, and consequently, the floatability of ZnS decreased due to the limited amount of PbS-like compounds formed on the ZnS surface by lead activation. Finally, cementation using ZVI could recover Pb^{2+} extracted from PbSO$_4$ during EDTA pretreatment as Pb^0, which will not only add economic value but also protect the environment.

Based on the findings of this study, a sustainable process flowsheet for complex sulfide ores is proposed (Figure 10). In this proposed flowsheet, PbSO$_4$ is first extracted by EDTA pretreatment before flotation. The residue obtained after EDTA pretreatment is fed to a flotation stage where ZnS floatability is effectively depressed by the conventional depressant for ZnS due to the decrease in the ratio of Pb^{2+}/Zn^{2+} of the flotation pulp, and then gangue minerals like SiO$_2$ and FeS$_2$ would be disposed of into a tailings dam after the recovery of ZnS with the assistance of activators (e.g., CuSO$_4$). Meanwhile, the leachate obtained from EDTA pretreatment is rich in Pb^{2+} that can be recovered via cementation using ZVI as Pb^0. To keep up with the high demand for critical metals following the SDGs, mine developments should be in harmony with the environment. This proposed flowsheet can achieve enhanced selective flotation of complex sulfide ores (depression of ZnS floatability) while preventing lead pollution to the surrounding environment of tailings dams (removal of toxic PbSO$_4$ before flotation) and maximizing the recovery of critical elements by cementation (recovery of Pb^0 using ZVI).
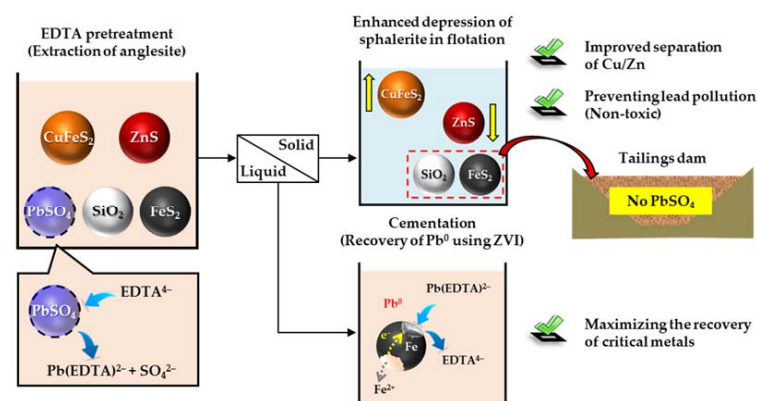
Figure 10. Proposed enhanced depression of sphalerite (ZnS) by extracting anglesite (PbSO$_4$) using ethylene diamine tetra acetic acid (EDTA) and recovery of the extracted Pb^{2+} as zero-valent Pb (Pb^0) by cementation using zero-valent Fe (ZVI).

4. Conclusions

In this paper, a pretreatment of flotation to extract $PbSO_4$ for the prevention of lead pollution to the surrounding environment of tailings dams and the depression of ZnS floatability combined with the recovery of extracted Pb^{2+} by cementation was investigated, and the findings of this study are summarized as follows:

1. ZnS floatability increased in the presence of $PbSO_4$.
2. The conventional depressants for ZnS, zinc sulfate and sodium sulfite, were not effective in depressing the floatability of ZnS when $PbSO_4$ was present.
3. Almost of all $PbSO_4$ (>97%) was extracted using EDTA, and >97% of the extracted Pb^{2+} could be recovered as Pb^0 by cementation using ZVI.
4. A pretreatment of flotation extracting $PbSO_4$ using EDTA was effective in depressing ZnS floatability.
5. The proposed method for complex sulfide ores containing $PbSO_4$, a combination of extraction of $PbSO_4$ using EDTA and recovery of extracted Pb^{2+} as zero-valent Pb by cementation using ZVI, could achieve enhanced selective flotation of complex sulfide ores (depression of ZnS floatability) while preventing lead pollution to the surrounding environment of tailings dams (removal of toxic $PbSO_4$ before flotation) and maximizing the recovery of critical elements by cementation (recovery of Pb^0 using ZVI).

Author Contributions: Conceptualization, K.A., M.I. and N.H.; methodology, K.A.; investigation, A.K.; data curation, A.K. and S.J.; writing—original draft preparation, K.A.; writing—review and editing, M.I., S.J., I.P. and N.H.; visualization, K.A.; supervision, N.H.; project administration, K.A.; funding acquisition, K.A. All authors have read and agreed to the published version of the manuscript.

Data Availability Statement: Not applicable.

References

1. Hák, T.; Janoušková, S.; Moldan, B. Sustainable Development Goals: A Need for Relevant Indicators. *Ecol. Indic.* **2016**, *60*, 565–573. [CrossRef]
2. Tabelin, C.B.; Park, I.; Phengsaart, T.; Jeon, S.; Villacorte-Tabelin, M.; Alonzo, D.; Yoo, K.; Ito, M.; Hiroyoshi, N. Copper and Critical Metals Production from Porphyry Ores and E-Wastes: A Review of Resource Availability, Processing/Recycling Challenges, Socio-Environmental Aspects, and Sustainability Issues. *Resour. Conserv. Recycl.* **2021**, *170*, 105610. [CrossRef]
3. Park, I.; Kanazawa, Y.; Sato, N.; Galtchandmani, P.; Jha, M.K.; Tabelin, C.B.; Jeon, S.; Ito, M.; Hiroyoshi, N. Beneficiation of Low-grade Rare Earth Ore from Khalzan Buregtei Deposit (Mongolia) by Magnetic Separation. *Minerals* **2021**, *11*, 1432. [CrossRef]
4. Goal 13 | Department of Economic and Social Affairs. Available online: https://sdgs.un.org/goals/goal13 (accessed on 26 April 2022).
5. Nansai, K.; Nakajima, K.; Kagawa, S.; Kondo, Y.; Suh, S.; Shigetomi, Y.; Oshita, Y. Global Flows of Critical Metals Necessary for Low-Carbon Technologies: The Case of Neodymium, Cobalt, and Platinum. *Environ. Sci. Technol.* **2014**, *48*, 1391–1400. [CrossRef] [PubMed]
6. WBG Minerals for Climate Action: The Mineral Intensity of the Clean Energy Transition. Available online: https://pubdocs.worldbank.org/en/961711588875536384/Minerals-for-Climate-Action-The-Mineral-Intensity-of-the-Clean-Energy-Transition.pdf (accessed on 25 April 2022).
7. Bilal, M.; Ito, M.; Koike, K.; Hornn, V.; Ul Hassan, F.; Jeon, S.; Park, I.; Hiroyoshi, N. Effects of Coarse Chalcopyrite on Flotation Behavior of Fine Chalcopyrite. *Miner. Eng.* **2021**, *163*, 106776. [CrossRef]
8. Bilal, M.; Ito, M.; Akishino, R.; Bu, X.; Ul Hassan, F.; Park, I.; Jeon, S.; Aikawa, K.; Hiroyoshi, N. Heterogenous Carrier Flotation Technique for Recovering Finely Ground Chalcopyrite Particles Using Coarse Pyrite Particles as a Carrier. *Miner. Eng.* **2022**, *180*, 107518. [CrossRef]
9. Hornn, V.; Ito, M.; Shimada, H.; Tabelin, C.B.; Jeon, S.; Park, I.; Hiroyoshi, N. Agglomeration–Flotation of Finely Ground Chalcopyrite Using Emulsified Oil Stabilized by Emulsifiers: Implications for Porphyry Copper Ore Flotation. *Metals* **2020**, *10*, 912. [CrossRef]
10. Hornn, V.; Ito, M.; Shimada, H.; Tabelin, C.B.; Jeon, S.; Park, I.; Hiroyoshi, N. Agglomeration-Flotation of Finely Ground Chalcopyrite and Quartz: Effects of Agitation Strength during Agglomeration Using Emulsified Oil on Chalcopyrite. *Minerals* **2020**, *10*, 380. [CrossRef]
11. Hornn, V.; Ito, M.; Yamazawa, R.; Shimada, H.; Tabelin, C.B.; Jeon, S.; Park, I.; Hiroyoshi, N. Kinetic Analysis for Agglomeration-Flotation of Finely Ground Chalcopyrite: Comparison of First Order Kinetic Model and Experimental Results. *Mater. Trans.* **2020**, *61*, 1940–1948. [CrossRef]

12. Hornn, V.; Park, I.; Ito, M.; Shimada, H.; Suto, T.; Tabelin, C.B.; Jeon, S.; Hiroyoshi, N. Agglomeration-Flotation of Finely Ground Chalcopyrite Using Surfactant-Stabilized Oil Emulsions: Effects of Co-Existing Minerals and Ions. *Miner. Eng.* **2021**, *171*, 107076. [CrossRef]

13. Park, I.; Hong, S.; Jeon, S.; Ito, M.; Hiroyoshi, N. A Review of Recent Advances in Depression Techniques for Flotation Separation of Cu–Mo Sulfides in Porphyry Copper Deposits. *Metals* **2020**, *10*, 1269. [CrossRef]

14. Park, I.; Hong, S.; Jeon, S.; Ito, M.; Hiroyoshi, N. Flotation Separation of Chalcopyrite and Molybdenite Assisted by Microencapsulation Using Ferrous and Phosphate Ions: Part I. Selective Coating Formation. *Metals* **2020**, *10*, 1667. [CrossRef]

15. Park, I.; Hong, S.; Jeon, S.; Ito, M.; Hiroyoshi, N. Flotation Separation of Chalcopyrite and Molybdenite Assisted by Microencapsulation Using Ferrous and Phosphate Ions: Part II. Flotation. *Metals* **2021**, *11*, 439. [CrossRef]

16. Seng, S.; Tabelin, C.B.; Makino, Y.; Chea, M.; Phengsaart, T.; Park, I.; Hiroyoshi, N.; Ito, M. Improvement of Flotation and Suppression of Pyrite Oxidation Using Phosphate-Enhanced Galvanic Microencapsulation (GME) in a Ball Mill with Steel Ball Media. *Miner. Eng.* **2019**, *143*, 105931. [CrossRef]

17. Aikawa, K.; Ito, M.; Kusano, A.; Park, I.; Oki, T.; Takahashi, T.; Furuya, H.; Hiroyoshi, N. Flotation of Seafloor Massive Sulfide Ores: Combination of Surface Cleaning and Deactivation of Lead-Activated Sphalerite to Improve the Separation Efficiency of Chalcopyrite and Sphalerite. *Metals* **2021**, *11*, 253. [CrossRef]

18. Ministry of Economic, Trade and Industry (METI) and Japan Oil, Gas and Metals National Corporation (JOGMEC). Summary Report on Comprehensive Evaluations of Development Plan of Seafloor Massive Sulfide Deposits. Available online: http://www.jogmec.go.jp/content/300359550.pdf (accessed on 26 February 2021).

19. Zeng, Z.; Chen, Z.; Qi, H. Two Processes of Anglesite Formation and a Model of Secondary Supergene Enrichment of Bi and Ag in Seafloor Hydrothermal Sulfide Deposits. *J. Mar. Sci. Eng.* **2021**, *10*, 35. [CrossRef]

20. Woodcock, J.T.; Sparrow, G.J.; Bruckard, W.J.; Johnson, N.W.; Dunne, R. *Plant Practice: Sulfide Minerals and Precious Metals. InFroth Flotation a Century of Innovation*; Fuerstenau, M., Jameson, G., Yoon, R.H., Eds.; SME: Littleton, CO, USA, 2007; pp. 781–843, ISBN 978-0-873-35252-9.

21. Wills, B.A.; Finch, J.A. Froth flotation. In *Mineral Processing Technology: An Introduction to the Practical Aspects of Ore Treatment and Mineral Recovery*, 8th ed.; Elsevier: Oxford, UK, 2016; pp. 265–380, ISBN 9780080970530.

22. Ball, J.W.; Nordstrom, D.K. *User's Manual for WATEQ4F, with Revised Thermodynamic Data Base and Text Cases for Calculating Speciation of Major, Trace, and Redox Elements in Natural Waters*; USGS Numbered Series Open-File Report 91-183; U.S. Geological Survey: Reston, VA, USA, 1991.

23. Rashchi, F.; Sui, C.; Finch, J.A. Sphalerite Activation and Surface Pb Ion Concentration. *Int. J. Miner. Process.* **2002**, *67*, 43–58. [CrossRef]

24. Laskowski, J.S.; Liu, Q.; Zhan, Y. Sphalerite Activation: Flotation and Electrokinetic Studies. *Miner. Eng.* **1997**, *10*, 787–802. [CrossRef]

25. Houot, R.; Raveneau, P. Activation of Sphalerite Flotation in the Presence of Lead Ions. *Int. J. Miner. Process.* **1992**, *35*, 253–271. [CrossRef]

26. Aikawa, K.; Ito, M.; Segawa, T.; Jeon, S.; Park, I.; Tabelin, C.B.; Hiroyoshi, N. Depression of Lead-Activated Sphalerite by Pyrite via Galvanic Interactions: Implications to the Selective Flotation of Complex Sulfide Ores. *Miner. Eng.* **2020**, *152*, 106367. [CrossRef]

27. Trahar, W.J.; Senior, G.D.; Heyes, G.W.; Creed, M.D. The Activation of Sphalerite by Lead—A Flotation Perspective. *Int. J. Miner. Process.* **1997**, *49*, 121–148. [CrossRef]

28. Rashchi, F.; Dashti, A.; Arabpour-Yazdi, M.; Abdizadeh, H. Anglesite Flotation: A Study for Lead Recovery from Zinc Leach Residue. *Miner. Eng.* **2005**, *18*, 205–212. [CrossRef]

29. Fuerstenau, M.C.; Olivas, S.A.; Herrera-Urbina, R.; Han, K.N. The Surface Characteristics and Flotation Behavior of Anglesite and Cerussite. *Int. J. Miner. Process.* **1987**, *20*, 73–85. [CrossRef]

30. Silwamba, M.; Ito, M.; Hiroyoshi, N.; Tabelin, C.B.; Hashizume, R.; Fukushima, T.; Park, I.; Jeon, S.; Igarashi, T.; Sato, T.; et al. Alkaline Leaching and Concurrent Cementation of Dissolved Pb and Zn from Zinc Plant Leach Residues. *Minerals* **2022**, *12*, 393. [CrossRef]

31. Schindler, M.; Santosh, M.; Dotto, G.; Silva, L.F.O.; Hochella, M.F. A Review on Pb-Bearing Nanoparticles, Particulate Matter and Colloids Released from Mining and Smelting Activities. *Gondwana Res.* **2021**. [CrossRef]

32. Park, I.; Tabelin, C.B.; Seno, K.; Jeon, S.; Inano, H.; Ito, M.; Hiroyoshi, N. Carrier-Microencapsulation of Arsenopyrite Using Al-Catecholate Complex: Nature of Oxidation Products, Effects on Anodic and Cathodic Reactions, and Coating Stability under Simulated Weathering Conditions. *Heliyon* **2020**, *6*, e03189. [CrossRef] [PubMed]

33. Shirley, D.A. High-Resolution X-ray Photoemission Spectrum of the Valence Bands of Gold. *Phys. Rev. B* **1972**, *5*, 4709–4714. [CrossRef]

34. Tabelin, C.B.; Corpuz, R.D.; Igarashi, T.; Villacorte-Tabelin, M.; Ito, M.; Hiroyoshi, N. Hematite-Catalysed Scorodite Formation as a Novel Arsenic Immobilisation Strategy under Ambient Conditions. *Chemosphere* **2019**, *233*, 946–953. [CrossRef] [PubMed]

35. Zoleta, J.B.; Itao, G.B.; Resabal, V.J.T.; Lubguban, A.A.; Corpuz, R.D.; Ito, M.; Hiroyoshi, N.; Tabelin, C.B. Improved Pyrolysis Behavior of Ammonium Polyphosphate-Melamine-Expandable (APP-MEL-EG) Intumescent Fire Retardant Coating System Using Ceria and Dolomite as Additives for I-Beam Steel Application. *Heliyon* **2020**, *6*, e03119. [CrossRef]

36. Silwamba, M.; Ito, M.; Hiroyoshi, N.; Tabelin, C.B.; Hashizume, R.; Fukushima, T.; Park, I.; Jeon, S.; Igarashi, T.; Sato, T.; et al. Recovery of Lead and Zinc from Zinc Plant Leach Residues by Concurrent Dissolution-Cementation Using Zero-Valent Aluminum in Chloride Medium. *Metals* **2020**, *10*, 531. [CrossRef]

37. Bicak, O. A Technique to Determine Ore Variability in a Sulphide Ore. *Miner. Eng.* **2019**, *142*, 105927. [CrossRef]

38. Grano, S.R.; Ralston, J.; Johnson, N.W. Characterization and Treatment of Heavy Medium Slimes in the Mt. Isa Mines Lead-Zinc Concentrator. *Miner. Eng.* **1988**, *1*, 137–150. [CrossRef]

39. Kant, C.; Rao, S.R.; Finch, J.A. Distribution of Surface Metal Ions among the Products of Chalcopyrite Flotation. *Miner. Eng.* **1994**, *7*, 905–916. [CrossRef]

40. Rumball, J.A.; Richmond, G.D. Measurement of Oxidation in a Base Metal Flotation Circuit by Selective Leaching with EDTA. *Int. J. Miner. Process.* **1996**, *48*, 1–20. [CrossRef]

41. Choi, S.; Jeon, S.; Park, I.; Ito, M.; Hiroyoshi, N. Addition of Fe_3O_4 as Electron Mediator for Enhanced Cementation of Cd^{2+} and Zn^{2+} on Aluminum Powder from Sulfate Solutions and Magnetic Separation to Concentrate Cemented Metals from Cementation Products. *J. Environ. Chem. Eng.* **2021**, *9*, 106699. [CrossRef]

42. Jeon, S.; Bright, S.; Park, I.; Tabelin, C.B.; Ito, M.; Hiroyoshi, N. The Effects of Coexisting Copper, Iron, Cobalt, Nickel, and Zinc Ions on Gold Recovery by Enhanced Cementation via Galvanic Interactions between Zero-Valent Aluminum and Activated Carbon in Ammonium Thiosulfate Systems. *Metals* **2021**, *11*, 1352. [CrossRef]

43. Choi, S.; Jeon, S.; Park, I.; Ito, M.; Hiroyoshi, N. Enhanced Cementation of Co^{2+} and Ni^{2+} from Sulfate and Chloride Solutions Using Aluminum as an Electron Donor and Conductive Particles as an Electron Pathway. *Metals* **2021**, *11*, 248. [CrossRef]

44. Jeon, S.; Tabelin, C.B.; Park, I.; Nagata, Y.; Ito, M.; Hiroyoshi, N. Ammonium Thiosulfate Extraction of Gold from Printed Circuit Boards (PCBs) of End-of-Life Mobile Phones and Its Recovery from Pregnant Leach Solution by Cementation. *Hydrometallurgy* **2020**, *191*, 105214. [CrossRef]

45. Jeon, S.; Tabelin, C.B.; Takahashi, H.; Park, I.; Ito, M.; Hiroyoshi, N. Enhanced Cementation of Gold via Galvanic Interactions Using Activated Carbon and Zero-Valent Aluminum: A Novel Approach to Recover Gold Ions from Ammonium Thiosulfate Medium. *Hydrometallurgy* **2020**, *191*, 105165. [CrossRef]

46. Jeon, S.; Bright, S.; Park, I.; Kuze, A.; Ito, M.; Hiroyoshi, N. A Kinetic Study on Enhanced Cementation of Gold Ions by Galvanic Interactions between Aluminum (Al) as an Electron Donor and Activated Carbon (AC) as an Electron Mediator in Ammonium Thiosulfate System. *Minerals* **2022**, *12*, 91. [CrossRef]

47. Jeon, S.; Bright, S.; Park, I.; Tabelin, C.B.; Ito, M.; Hiroyoshi, N. A Simple and Efficient Recovery Technique for Gold Ions from Ammonium Thiosulfate Medium by Galvanic Interactions of Zero-Valent Aluminum and Activated Carbon: A Parametric and Mechanistic Study of Cementation. *Hydrometallurgy* **2022**, *208*, 105815. [CrossRef]

48. Choi, S.; Yoo, K.; Alorro, R.D.; Tabelin, C.B. Cementation of Co Ion in Leach Solution Using Zn Powder Followed by Magnetic Separation of Cementation-Precipitate for Recovery of Unreacted Zn Powder. *Miner. Eng.* **2020**, *145*, 106061. [CrossRef]

49. Choi, S.; Jeon, S.; Park, I.; Tabelin, C.B.; Ito, M.; Hiroyoshi, N. Enhanced Cementation of Cd^{2+}, Co^{2+}, Ni^{2+}, and Zn^{2+} on Al from Sulfate Solutions by Activated Carbon Addition. *Hydrometallurgy* **2021**, *201*, 105580. [CrossRef]

50. Silwamba, M.; Ito, M.; Tabelin, C.B.; Park, I.; Jeon, S.; Takada, M.; Kubo, Y.; Hokari, N.; Tsunekawa, M.; Hiroyoshi, N. Simultaneous Extraction and Recovery of Lead Using Citrate and Micro-Scale Zero-Valent Iron for Decontamination of Polluted Shooting Range Soils. *Environ. Adv.* **2021**, *5*, 100115. [CrossRef]

51. Xi, Y.; Mallavarapu, M.; Naidu, R. Reduction and Adsorption of Pb^{2+} in Aqueous Solution by Nano-Zero-Valent Iron—A SEM, TEM and XPS Study. *Mater. Res. Bull.* **2010**, *45*, 1361–1367. [CrossRef]

52. Taylor, J.A.; Perry, D.L. An X-ray Photoelectron and Electron Energy Loss Study of the Oxidation of Lead. *J. Vac. Sci. Technol. A Vac. Surf. Film.* **1998**, *2*, 771. [CrossRef]

53. Silwamba, M.; Ito, M.; Hiroyoshi, N.; Tabelin, C.B.; Fukushima, T.; Park, I.; Jeon, S.; Igarashi, T.; Sato, T.; Nyambe, I.; et al. Detoxification of Lead-Bearing Zinc Plant Leach Residues from Kabwe, Zambia by Coupled Extraction-Cementation Method. *J. Environ. Chem. Eng.* **2020**, *8*, 104197. [CrossRef]

54. El-Shall, H.E.; Elgillani, D.A.; Abdel-Khalek, N.A. Role of Zinc Sulfate in Depression of Lead-Activated Sphalerite. *Int. J. Miner. Process.* **2000**, *58*, 67–75. [CrossRef]

55. Basilio, C.I.; Kartio, I.J.; Yoon, R.-H. Lead Activation of Sphalerite during Galena Flotation. *Miner. Eng.* **1996**, *9*, 869–879. [CrossRef]

56. Helgeson, H.C. Thermodynamics of Hydrothermal Systems at Elevated Temperatures and Pressures. *Am. J. Sci.* **1969**, *267*, 729–804. [CrossRef]

57. Latimer, W.M. *The Oxidation States of the Elements and Their Potentials in Aqueous Solutions*, 2nd ed.; Prentice-Hall, Inc.: Upper Saddle River, NJ, USA, 1952; pp. 72, 152, 169, ISBN 978-0-758-15876-5.

58. Leckie, J.O.; James, R.O. *Aqueous Environmental Chemistry of Metals*; Rubin, A.J., Ed.; Ann Arbor Science Publishers: Ann Arbor, MI, USA, 1974; pp. 1–76, ISBN 978-0-250-40060-7.

59. Liu, J.; Ejtemaei, M.; Nguyen, A.V.; Wen, S.; Zeng, Y. Surface Chemistry of Pb-Activated Sphalerite. *Miner. Eng.* **2020**, *145*, 106058. [CrossRef]

60. Hernan, L.; Morales, J.; Sanchez, L.; Tirado, J.L.; Espinos, J.P.; Gonzalez Elipe, A.R. Diffraction and XPS Studies of Misfit Layer Chalcogenides Intercalated with Cobaltocene. *Chem. Mater.* **1995**, *7*, 1576–1582. [CrossRef]